Virginia Tech Helmet Lab
343 Kelly Hall
325 Stanger St
Blacksburg, Virginia 24061
P: (540) 231-8254
rowson@vt.edu

Equestrian STAR Protocol

Lauren A. Duma, Mark Begonia, Barry Miller, and Steve Rowson

Laboratory Tests

A pendulum impactor and oblique drop tower are used in impact testing because both linear-driven and oblique impacts are possible in equestrian environments. The pendulum impactor uses a pendulum arm that is 190.5 cm long, has a total mass of 36.3 kg with a 16.3 kg impacting mass at the end, and has a moment of inertia of 72 kg·m2 (Figure 1) [1]. A flat, rigid nylon impactor face with a 12.7 cm diameter and 2.5 cm thickness is used to minimize any differences between helmets in comparative testing due to impactor compliance. The pendulum impacts a helmeted, medium NOCSAE headform, which is modified to fit a 50th percentile male Hybrid III neck. The head and neck are mounted to a 5-degree-of-freedom Biokinetics slide table with a 16 kg sliding mass. This setup allows for linear and rotational motion to be generated during an impact and is representative of the head, neck, and torso of a 50th percentile male. Test conditions include three impact locations (front, side, and back) and two impact speeds (4.0 and 6.3 m/s), resulting in a total of six test configurations (Figure 2, Table 1) [2, 3]. Helmet position on the headform is set according to fitting guidelines provided by the manufacturer. Four samples of each helmet model are subjected to one impact per location at a given speed. Two trials are performed at each of the six test configurations, producing a total of 12 pendulum impacts per helmet model.

Figure 1: Pendulum impactor used for Equestrian STAR testing.

Figure 2: Impact locations used in pendulum testing: front, side, and back.

Table 1: Relative NOCSAE headform translations and rotations on the linear slide table for each impact configuration.

Location	Y (cm)	Z (cm)	Ry (deg)	Rz (deg)
Front	0	+0.8	-30°	0°
Side	-1	+4.8	-10°	-100°
Back	0	+6.3	0°	180°

Notes: All measurements are made using the SAE J211 coordinate system in relation to a "zero" condition in which the headform is in a position of 0° Y and Z-axis rotation and the median (midsagittal) and basic (transverse) plane intersection of the headform is aligned with the center of the impactor. The x-position is set such that the helmet barely contacts the impactor face when the pendulum arm is in a neutral vertical position for each location.

Oblique testing is performed on an oblique drop tower (Figure 3). A 45° steel anvil produces normal and tangential incident velocities associated with oblique impacts. The anvil is coated with 80-grit sandpaper, which is replaced after every fourth test. For each test, a helmeted medium NOCSAE headform is positioned in a support ring connected to the drop tower and secured in place with a lever arm that is released just prior to impact. The support ring passes around the outside of the anvil upon impact. No anthropomorphic test device (ATD) neck or effective torso mass is used in testing, as previous work has suggested that oblique impacts may subject the neck to considerable axial loading, a scenario known to present limited biofidelity for current ATD necks [4-6].

Test conditions include four impact locations (left front boss, right front boss, left rear boss, and right rear boss) and one impact speed (6.56 m/s), for a total of four oblique impacts per helmet model (Tables 2 and 3). Data from the left and right front boss are averaged into one value for the front boss, and data from the left and right rear boss are averaged into one value for the rear boss. As each location is only impacted once, only one helmet is acquired and tested for each helmet model. Impact locations are spaced a minimum distance of 120 mm apart to avoid overlap of damage profiles [7]. Headform position in the support ring is specified using an inclinometer mounted on a custom holder that fits inside the NOSCAE instrumentation channel. The inclinometer base faces the neck region of the headform and lays parallel to the base of the headform (2.5° offset from the Frankfort plane). Z rotation is verified with a cross-level laser and 5° increments inscribed on the support ring.

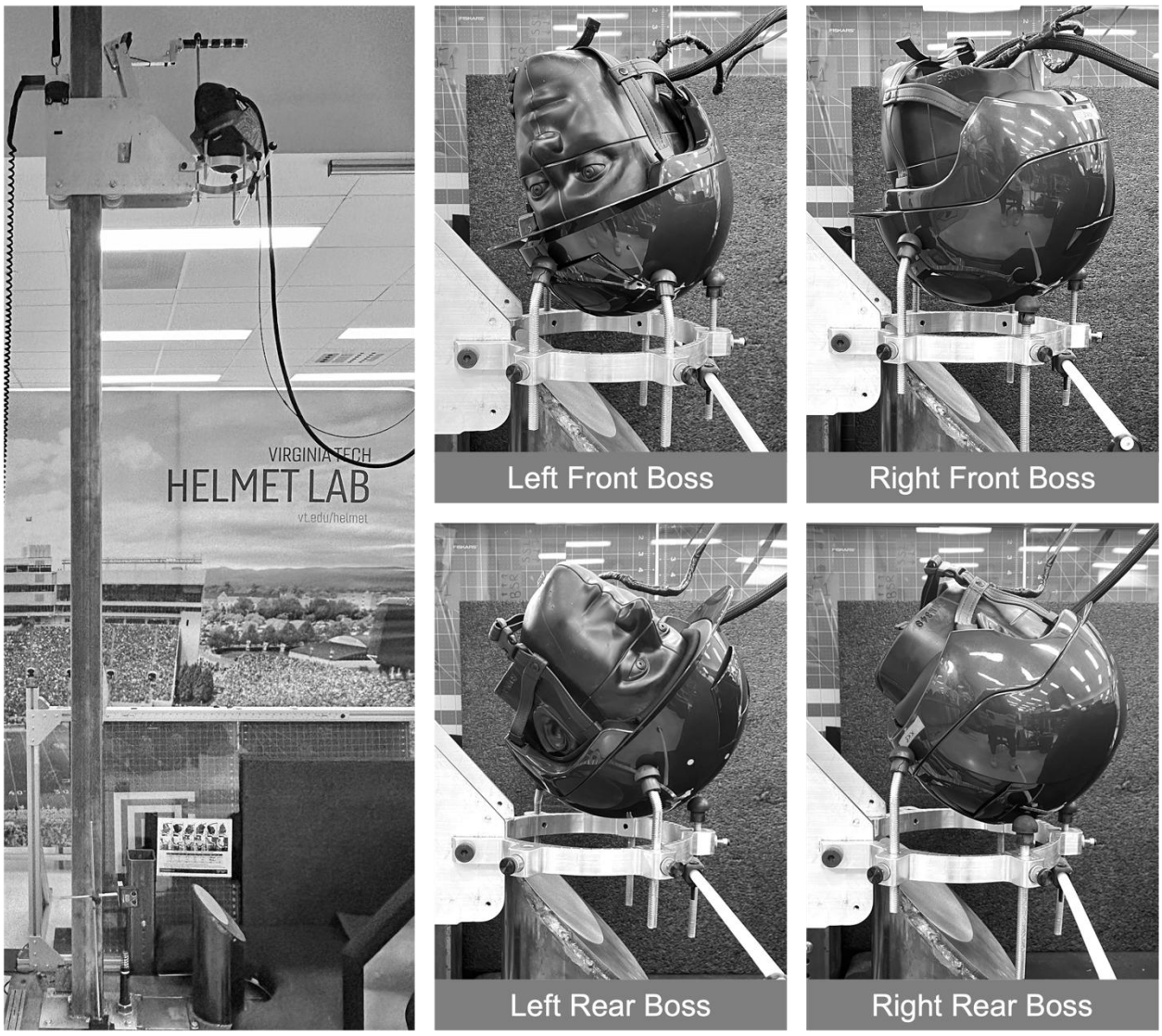

Figure 3: The oblique drop tower and four impact locations used in oblique testing (front boss is the average of left and right front boss, rear boss is the average of left and right rear boss).

Table 2: NOCSAE headform rotations on the support ring for each oblique impact location.

Location		X (deg)	Y (deg)	Z (deg)
Front boss	Left	15.6°	5.7°	-80°
	Right	-15.6°	5.7°	80°
Rear boss	Left	46.0°	-27.9°	170°
	Right	-46.0°	-27.9°	-170°

Notes: X and Y rotations were determined with an inclinometer according to the SAE J211 coordinate system, and Z axis rotation was determined by projecting the midsagittal line (for front boss locations) or midcoronal line (for rear boss locations) of the headform face onto the support ring marked with 5° increments. A 0° position corresponds to the headform facing the drop tower, with positive Z values increasing in the clockwise direction and negative in the counterclockwise direction.

Table 3: Impact velocity for oblique testing, including the resultant, normal, and tangential components. This velocity was chosen based on recommendations from the FEI.

Resultant Velocity (m/s)	Normal Velocity (m/s)	Tangential Velocity (m/s)
6.56	4.64	4.64

For both the pendulum impactor and oblique drop tower, the NOCSAE headform is instrumented with three linear accelerometers and a triaxial angular rate sensor (ARS) at its center of gravity to measure linear and rotational impact kinematics. Data are sampled at 20,000 Hz and filtered using a 4-pole Butterworth low pass filter with a cutoff frequency of 1650 Hz (CFC 1000) for accelerometer data and 300 Hz (CFC 180) for ARS data. Rotational accelerations are calculated through five-point stencil differentiation of the angular rate data. Peak resultant linear acceleration and peak resultant rotational acceleration are then used to estimate risk of concussion. Risks are averaged together per impact configuration to compute Summation of Tests for the Analysis of Risk (STAR) values.

STAR Ratings

The STAR equation was originally developed to estimate the incidence of concussion that a college football player may experience while wearing a given helmet over the course of one season [8]. Common real-world impacts are simulated using laboratory testing, with the resulting concussion risk for each impact estimated and then weighted based on the relative frequency that a player might experience that impact scenario (termed "exposure"). The STAR value is found by multiplying the predicted on-field exposure (E) at each impact location (L) and velocity (V) by the risk of concussion (R) for that impact. Concussion risk is modeled using the peak resultant linear acceleration (a) and rotational acceleration (α) from laboratory impacts. The overall Equestrian STAR equation is broken into two equations, one for pendulum impactor testing and a second for oblique drop tower testing (Equations 1, 2, and 3).

$$Equestrian\ STAR = Equestrian\ STAR_{pendulum} + Equestrian\ STAR_{oblique} \quad \text{(Eq. 1)}$$

$$Equestrian\ STAR_{pendulum} = \sum_{L=1}^{3}\sum_{V=1}^{2} E(L,V) * R(a,\propto) \quad \text{(Eq. 2)}$$

$$Equestrian\ STAR_{oblique} = \sum_{L=1}^{2}\sum_{V=1}^{1} E(L,V) * R(a,\propto) \quad \text{(Eq. 3)}$$

Concussion risk was modeled using a multivariate logistic regression analysis of biomechanical data obtained from instrumented football players who sustained diagnosed concussions [9]. The associated risk function combines peak linear head acceleration (PLA) and peak rotational head acceleration (PRA), which are both known to be associated with brain injury, into a single metric (Equation 4) [10].

$$R(a,\alpha) = \frac{1}{1 + e^{-(-10.2 + 0.0433*a + 0.000873*\alpha - 0.00000092*a\alpha)}} \quad \text{(Eq. 4)}$$

Exposure values for each impact configuration were assigned using a video analysis of equestrian falls and previously published equestrian fall data [1-2, 11] (Table 4). Because locations across equestrian helmets are impacted in similar frequencies during equestrian falls, each impact location was treated as having a similar exposure. The low-speed impact conditions were assigned an exposure value of three because equestrian falls from lower, reduced fall heights occur approximately three times as frequently.

Table 4: Exposure values for each configuration, which are used as weightings to obtain a STAR Score for each helmet model.

Location	Pendulum		Oblique
	4.0 m/s	6.3 m/s	6.3 m/s
Front	3	1	*n/a*
Side	3	1	*n/a*
Back	3	1	*n/a*
Front boss	*n/a*	*n/a*	1
Rear boss	*n/a*	*n/a*	1

The range of final STAR scores across helmets were then distributed into a discrete number of stars (1 to 5) for consumer interpretation (Table 5). Lower scores (i.e., lower concussion risk) are associated with a higher rating and representative of better performing helmets.

The Equestrian STAR rating thresholds were determined through the average STAR score across all tested helmets. A 5-star rating threshold was set to a 50% reduction in STAR score relative to the mean STAR score for equestrian helmets, and then each subsequent rating threshold was set in increments of 50% more risk from the 5-star threshold (Table 5). For example, the 4-star threshold is 1.5 times the 5-star threshold, and the 3-star threshold is two times the 5-star threshold.

Table 5: Thresholds to match STAR values to number of stars in a 5-star rating scale.

STAR Score	Number of Stars
< 2.45	5
< 3.67	4
< 4.90	3
< 6.12	2
< 7.34	1
≥ 7.34	0

References

[1] Rowson, B., S. Rowson, and S. M. Duma. Hockey star: A methodology for assessing the biomechanical performance of hockey helmets. *Annals of Biomedical Engineering* 43: 2429-43, 2015. https://doi.org/10.1007/s10439-015-1278-7

[2] Connor, T. A., J. M. Clark, M. Stewart, A. N. Annaidh, and M. D. Gilchrist. Post-accident evidence basis for new equestrian standards: Relationship between helmet liner residual crush and accident parameters. *Applications in Engineering Science* 6: 100044, 2021. https://doi.org/10.1016/j.apples.2021.100044

[3] Clark, J. M., C. Williams, J. Clissold, A. McGoldrick, J. Hill, A. N. Annaidh, and M. D. Gilchrist. Video analysis of head injury incidents in equestrian sports. *Sports Engineering* 23: 10, 2020. https://doi.org/10.1007/s12283-020-00323-0

[4] Bland, M.L., C. McNally, and S. Rowson. Headform and Neck Effects on Dynamic Response in Bicycle Helmet Oblique Impact Testing. Proceedings of IRCOBI Conference, 2018. Athens, Greece. https://www.ircobi.org/wordpress/downloads/irc18/pdf-files/69.pdf

[5] Sances, A.J., F. Carlin, and S. Kumaresan. Biomechanical analysis of head-neck force in Hybrid III dummy during inverted vertical drops. *Biomedical sciences instrumentation* 38: 459-464, 2002.

[6] Rousseau, P., T.B. Hoshizaki, and M.D. Gilchrist. Estimating the influence of neckform compliance on brain tissue strain during a helmeted impact. *Stapp Car Crash Journal* 54: 37-48, 2010. https://doi.org/10.4271/2010-22-0003

[7] CPSC. Safety standard for bicycle helmets final rule (16 cfr part 1203). United States Consumer Product Safety Commission. 11711-11747, 1998.

[8] Rowson, S. and S. M. Duma. Development of the STAR evaluation system for football helmets: Integrating player head impact exposure and risk of concussion. *Annals of Biomedical Engineering* 39: 2130-40, 2011. https://doi.org/10.1007/s10439-011-0322-5

[9] Rowson, S. and S. M. Duma. Brain injury prediction: Assessing the combined probability of concussion using linear and rotational head acceleration. *Annals of Biomedical Engineering* 41: 873-82, 2013. https://doi.org/10.1007/s10439-012-0731-0

[10] Ommaya, A.K. Biomechanics of Head Injuries: Experimental Aspects. *Biomechanics of Trauma*, A. Nahum, J. W. Melvin, Ed. Eat Norwalk, CT: Appleton-Century-Crofts, 1985.

[11] Duma, L.A., M.T. Begonia, B. Miller, C. Jung, M. Wood, B.G. Duma, and S. Rowson. Equestrian STAR: Development of an Experimental Methodology for Assessing the Biomechanical Performance of Equestrian Helmets. Annals of Biomedical Engineering 1-24, 2025. https://doi.org/10.1007/s10439-025-03723-0